06

Effect of synthesis conditions on the structure and electronic properties of diamond-like carbon films with iridium nanoparticles

© F. Bekmurat,[1,2] A.P. Ryaguzov,[1] R.R. Nemkayeva,[1] A.R. Assembayeva,[1,3] N.R. Guseinov,[1] R.Zh. Yersaiyn[4]

[1] National nanotechnology laboratory of open type, Al-Farabi Kazakh National University,
050012 Almaty, Kazakhstan
[2] Department of Solid State Physics and Technology of New Materials, Al-Farabi KazNU,
[3] Kazakh National Technical Research University,
050000 Almaty, Kazakhstan
[4] D.V.Sokolsky Institute of Fuel, Catalysis and Electrochemistry,
050010 Almaty, Kazakhstan
e-mail: zh.fariza1@mail.ru

Received October 28, 2024
Revised October 28, 2024
Accepted October 28, 2024

This study investigates the possibility of controlling the sp^2/sp^3 hybridized bond ratio in diamond-like carbon (DLC) films modified with iridium nanoparticles. The DLC films were synthesized by magnetron sputtering of a combined target. Surface morphology and elemental composition of the DLC films were studied using electron microscopy and EDS analysis. Scanning electron microscopy revealed that iridium forms nanoparticles within the carbon matrix. Raman spectroscopy was employed to investigate the local structure of amorphous DLC films depending on synthesis conditions and iridium concentration. The dependence of the G, D, and T peak positions on synthesis conditions and iridium concentration was demonstrated. The intensity ratio I_D/I_G was calculated, and changes in the full width at half maximum (FWHM) of the G peak as a function of iridium concentration were shown. Additionally, the shift of the G peak dispersion from a diamond-like to a graphite-like phase with increasing iridium concentration was observed. The value of bandgap of DLC films containing iridium nanoparticles was determined, and its dependence on synthesis conditions and iridium concentration was shown. Furthermore, percolation conductivity was observed in DLC films with iridium nanoparticles at an iridium concentration of 0.9 at.%.

Keywords: Magnetron sputtering, diamond-like carbon film, nanoparticle, iridium, Raman spectroscopy.

DOI: 10.61011/TP.2025.02.60836.364-24

Introduction

Diamond-like carbon (DLC) films are amorphous materials consisting of hybridized sp^1-, sp^2- and sp^3-bonds of carbon atoms [1]. Due to their low friction coefficient, high hardness, chemical inertness, and optical transparency, DLC films are used as coatings for critical devices and mechanisms [2–5].

DLC films are modified with various metals to reveal new properties and enable control over these properties. Modifiers in DLC films may affect internal stresses, microhardness, and elastic modulus to varying degrees. The deposition of DLC films with the incorporation of various metals can also significantly enhance their mechanical, tribological, and chemical properties.

Non-carbide-forming elements (e.g., Ag, Pt, Pd, Ir, Ni), which do not chemically bond with carbon under ambient conditions, lead to the formation of metal nanoparticles (NPs) within the amorphous carbon matrix. In Ref. [6], the influence of Cu nanoparticles on tribological properties is demonstrated, where it is reported that Cu NPs can reduce the coefficient of friction and significantly decrease the wear rate of the films. The corrosion protection efficiency also increases by 4% with the addition of silver to the DLC film [7]. Composite diamond-like carbon films modified with copper and tungsten [8] exhibit high hardness of 35 GPa and a low coefficient of friction of 0.14. The introduction of titanium at a concentration of 2.8 at.% into the DLC film enhances its adhesion strength [9]. The addition of nickel to DLC coatings [10] increases adhesion strength to substrates, enhances corrosion resistance, and improves wear resistance. Ref. [11] demonstrates that Pd NPs are promising as an effective additive for reducing the friction coefficient of DLC films.

The study of the electronic properties of DLC films is also of considerable importance. The ratio of sp^2 and sp^3-bonds present in DLC films significantly affects both their mechanical and electronic properties. The introduction of non-carbide-forming metals such as Cu, Ag, and Au [12] can significantly alter the electrical conductivity and optical properties of DLC films. In addition, an understanding of the electronic processes occurring under the influence of an electric field is essential. Understanding of their dependence on the modifier concentration and synthesis conditions is also important. For example, the specific electrical resistivity of diamond-like carbon films can be reduced by several

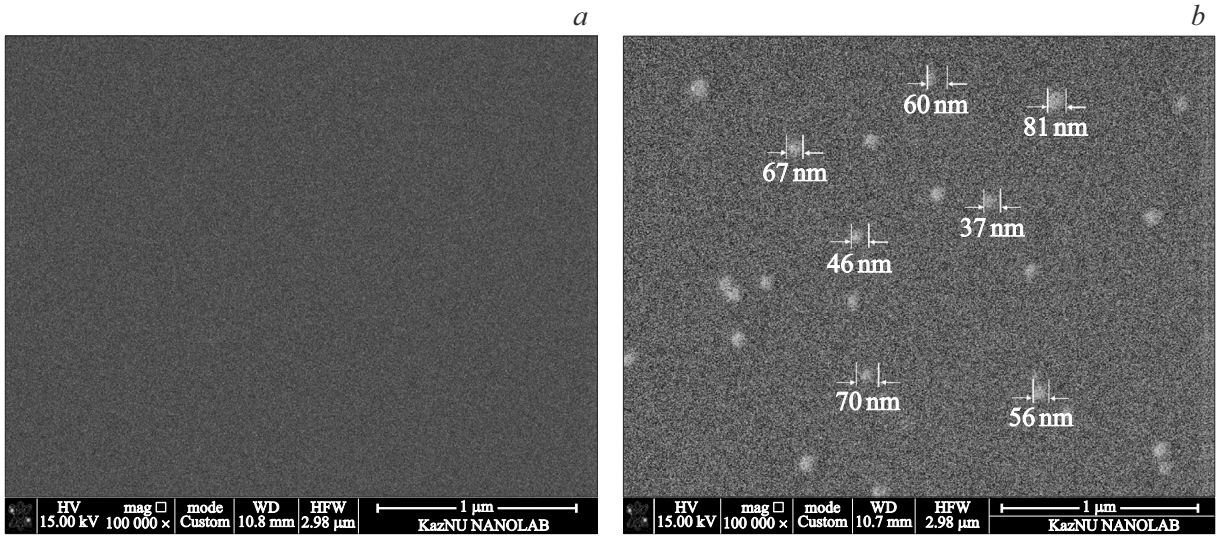

Figure 1. Scanning electron microscopy image of DLC films: X_{Ir}, at.%: *a* — 0.00, *b* — 3.50.

orders of magnitude through the incorporation of various metals into the film composition [13]. The band gap width of DLC films, determined in [14] and calculated using the Tauc retio, varied from 2.63 to 1.48 eV with increasing Ni concentration. The surface plasmon resonance of DLC : H films containing 10 at.% silver exhibits an intense absorption peak around 460 nm [15]. In the study by the authors [16], an increase in conductivity from $\sim 10^{-6}$ to 10^{2} S/cm was demonstrated with increasing palladium concentration in the range from 0.17 to 1 at.%. With the introduction of iridium, a percolation effect is also observed [17], i.e., the conductivity increases by a factor of 10^{7} at an iridium concentration of 0.7 at.%. In [18], the band gap decreases as the film thickness and content of Ni increase.

Iridium is underexplored as a nanoscale material. Similar to other noble metals, iridium attracts interest due to its unique physical, chemical, electronic and catalytic properties. Water-dispersible iridium nanoclusters (Ir NCs) [19] have better stability and extinction coefficient that is two orders of magnitude as high as that of Au nanoclusters. Moreover, as shown in Ref. [19], fluorescence is observed. The obtained data has high fundamental and applied significance. Iridium does not form chemical bonds with carbon during synthesis [20]; therefore, within the amorphous carbon matrix, iridium forms nanoparticles, analogous to the behavior of gold, silver, and other platinum-group elements. It is expected that modification of amorphous DLC films with iridium nanoparticles will affect the distribution of electron density of states in the band structure and, consequently, the electronic properties. Thus, introduction of iridium into diamond-like carbon films may reveal new properties of synthesized films and, thus, expand their range of applications.

DLC films are fabricated by various synthesis methods [21–24]. In this study, direct current (DC) magnetron sputtering of a composite target was used. The advantage of magnetron co-sputtering compared to other synthesis methods lies in its ability to control a number of key parameters, such as plasma current, voltage, and working gas pressure during the synthesis process.

1. Materials and procedure of the experiment

DLC films with iridium nanoparticles were synthesized using a TSU600 system (Beijing Technol CO., LTD, China) in an argon atmosphere (99.9999%) at a pressure of 0.7 Pa. The deposition of DLC⟨Ir⟩ films was carried out at DC plasma discharge powers of 17.5, 19.25, and 21 W on fused quartz and crystalline silicon (100) substrates (Changchun Yutai Optics Co., Ltd., China). The substrate temperature was controlled by a thermocouple and didn't exceed 50°C. A composite target was used, consisting of a polycrystalline carbon plate (99.9999 at.%) (Zhongnuo Xin Technology Co. Ltd., China) and iridium wire segments (99.9 at.%) (Sigma-Aldrich, USA), no longer than 5 mm, which were placed in the erosion zone. The substrates were cleaned in an ultrasonic bath of isopropanol and in a ternary mixture of $60H_2O+20H_2O_2+20HN_3OH$, followed by RF ion-plasma cleaning at a power of 15 W and a residual gas pressure of 21 Pa for 30 minutes.

The surface structure and the sizes of iridium nanoparticles were investigated using a Quattro C scanning electron microscope (Thermo Fisher Scientific, FEI, USA) at an accelerating voltage of 15 kV and a residual gas pressure of $1.15 \cdot 10^{-3}$ Pa. The SEM photograph in Figure 1, *a* shows that pure DLC films have a smooth surface without any structural features. At a DC discharge power of 17.5 W and an iridium concentration of 3.5 at.%, as shown in Fig. 1, *b*, brightness inhomogeneities of spherical shape appear in the carbon matrix, with sizes ranging from 37 to 81 nm.

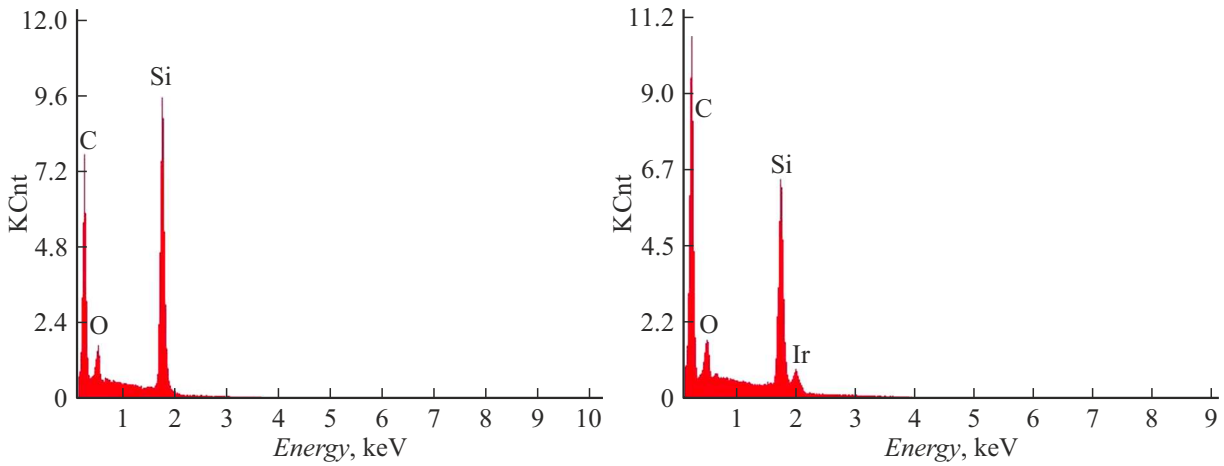

Figure 2. Energy-dispersive spectrum of DLC films at the DC discharge power of 17.5 W: X_{Ir}, at.%: *a* — 0.00, *b* — 3.50.

According to EDS analysis, these inhomogeneities can be identified as iridium nanoparticles.

The iridium concentration (X_{Ir}) in the DLC film matrix was measured by EDS using an EDAX analyzer (AMETEK Materials Analysis Division, USA) and varied in the range from 0 to 3.5 ± 0.03 at.% (Fig. 2). Energy-dispersive X-ray microanalysis was carried out at 4 kV and 6 kV on films deposited on silicon substrates. The EDS spectra of the pure amorphous DLC films shown in Fig. 2, *a* exhibit peaks corresponding to carbon, silicon, and oxygen. The addition of iridium results in the appearance of an iridium peak (Fig. 2, *b*). The EDS spectrum has no other peaks of foreign elements.

The effect of iridium concentration and synthesis conditions on the local structure of the films was investigated by Raman spectroscopy. RS was recorded on the Ntegra Spectra (NT-MDT, Russia) unit using 473 nm and 633 nm lasers. The exposure time was 100 s.

The optical band gap was determined based on transmission and reflection spectra obtained using a Lambda 35 spectrophotometer in the wavelength range from 190 to 1100 nm.

The study of electrical conductivity and its temperature dependence was carried out in electric fields with an intensity of $E \leq 5 \cdot 10^4$ V/cm, within the linear region of the current-voltage characteristics, using a planar electrode configuration. For numerical data analysis and plotting of curves, Origin2018 software was used.

2. Raman scattering

Raman scattering is a non-destructive method that enables the determination of the local structure of carbon films and the identification of changes in the ratio of sp^2/sp^3-hybridized bonds. The Raman scattering crosssection of sp^2-bonded sites in the visible range exceed that of sp^3-bonded sites by a factor of 50–250. This is attributed to the high mobility and polarizability of π-electrons, as well as the higher phonon density of states in sp^2-clusters [26]. All these differences enable the effective use of Raman scattering for the analysis and characterization of the structure of amorphous diamond-like carbon films.

The RS method was used to examine the influence of plasma discharge power and iridium concentration on the local structure of amorphous DLC films. Fig. 3 presents the Raman spectra of pure DLC films and those with the maximum iridium concentration, obtained at different discharge powers. The presented spectra are typical of amorphous carbon structures, with a full width at half maximum (FWHM) of the main peak equal to $\sim 200{-}250\,\mathrm{cm}^{-1}$. The Raman spectra of pure DLC films exhibit a single main peak centered near $1550\,\mathrm{cm}^{-1}$, with a shoulder in the low-frequency region around $1360\,\mathrm{cm}^{-1}$ (Fig. 3, *a*). Such a spectrum is characteristic of diamond-like carbon films containing more than 40% of sp^3-hybridized bonds [25–27]. Thus, the position of the main peak in the amorphous DLC film is determined by molecular structural units composed of $sp^2{-}sp^3$-bonds. As seen in Fig. 3, *a*, the intensity of the Raman spectra of pure DLC films decreases with increasing DC discharge power. In the spectra shown in Fig. 3, *b*, at an iridium concentration of $\approx 3.50 \pm 0.03$ at.%, the peak position also remains unchanged with varying DC discharge power and is located at $1540\,\mathrm{cm}^{-1}$. But a significant decrease in the RS spectra band frequency of DLC films with iridium can be also seen compared with pure amorphous DLC films. In addition, an increase in the intensity of the low-frequency shoulder at $1360\,\mathrm{cm}^{-1}$ relative to the main peak is observed upon the introduction of the modifier. Therefore, iridium affects structuring by reducing the number of structural units of DLC films, whose phonon spectrum is characterized by the frequency at $1540\,\mathrm{cm}^{-1}$. In all RS spectra of DLC films, a second-order peak is also observed at $3000\,\mathrm{cm}^{-1}$.

For detailed analysis of RS spectra, they were decomposed by the Voigt method (Figure 4). The Voigt distribution is a probability distribution obtained by the

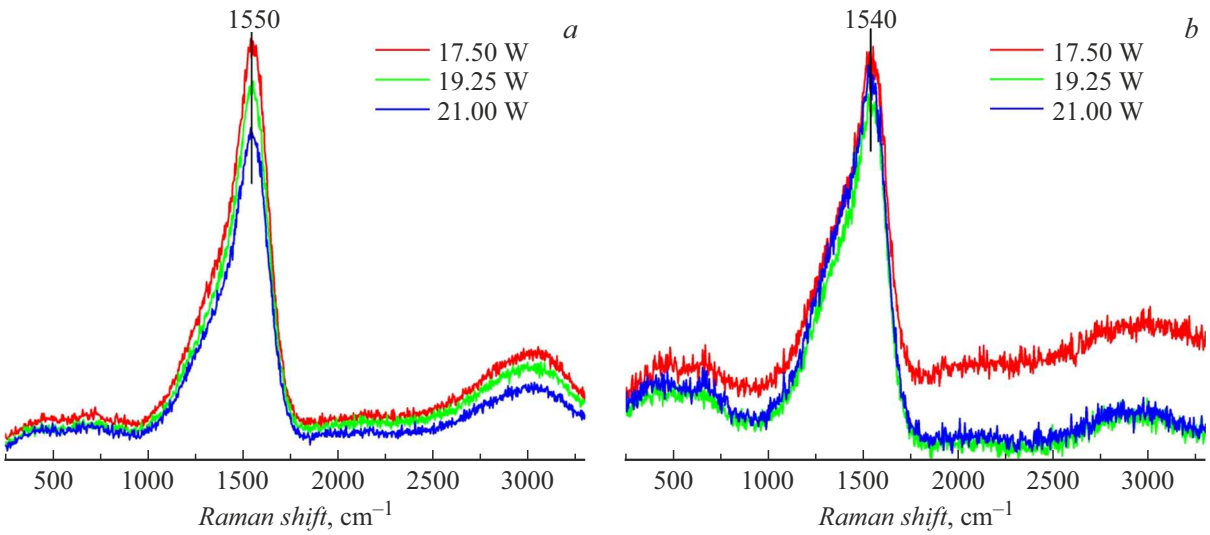

Figure 3. Raman scattering of DLC films deposited at different discharge powers and iridium concentration. X_{Ir}, at.%: *a* — 0.00, *b* — 3.50 ± 0.03.

convolution of a Lorentzian and a normal (Gaussian) distribution. Decomposition curves are green, a resulting curve is red, experimental data is shown as black dots. The decomposition was carried out using the minimum number of component peaks necessary to achieve the best fit between the resulting curve and the experimental data. In this case, the reliability of the fit was $R^2 > 0.99$. As a result, typical peaks G, D and T were obtained [1]. The G-peak corresponds to the stretching and compression of molecules originating from sp^2-units and is identified in the region of $1550-1555\,\mathrm{cm}^{-1}$. The D-peak is attributed to the vibrations of the hexagonal C_6 molecule, characterized by a breathing mode in the region of $1360-1390\,\mathrm{cm}^{-1}$. T-peak corresponds to the vibrations of sp^3 bonds of the tetragonal structure and is observed in the frequency range $1200-1260\,\mathrm{cm}^{-1}$. The peak position, intensity ratio (I_T/I_G, I_D/I_G), and full width at half maximum (FWHM) can be used to determine the ratio of sp^2/sp^3-hybridized bonds.

The positions of the G-peak maxima in the pure films, shown in Fig. 4, *a*–*c*, do not change significantly with increasing discharge power and are located at ~ 1550 cm. The introduction of iridium doesn't shift the position of the G-peak (Fig. 4, *d*–*f*); at the maximum concentration of $X_{\mathrm{Ir}} \sim 3.5$ at.% , it is located at $1552\,\mathrm{cm}^{-1}$ in the films deposited at 21 W.

The shift of the G-peak toward higher frequencies indicates an increased fraction of sp^2-sites in the structure [26]. At the same time, the area ratio of the G-peaks decreases by a factor of 2.8 with increasing iridium concentration in the films deposited at a discharge power of 17.5 W. With increasing discharge power, a 1.99-fold decrease in the area ratio of the G-peaks is observed with the growth of X_{Ir}.

In the pure films synthesized at 17.5 and 19.25 W, the position of the T-peak corresponds to $\sim 1260\,\mathrm{cm}^{-1}$. A further increase in power by 1.75 W shifts the position of the T-peak toward the low-frequency region, reaching $1255\,\mathrm{cm}^{-1}$. The introduction of iridium into the DLC film matrix significantly shifts the T-peak toward the low-frequency region. The maximum shift of the T-peak at the highest Ir concentration is observed at a discharge power of 21 W and reaches $1210\,\mathrm{cm}^{-1}$ (Fig. 4, *f*). A decrease in the area and intensity of the T-peak with increasing concentration up to 3.5 at.% can also be observed.

The D-peak position in films varies at $1372-1387\,\mathrm{cm}^{-1}$ depending on the synthesis conditions. In contrast to the intensities of the T- and G-peaks, the intensity and area of the D-peak increase with increasing X_{Ir}. The maximum increase in the D-peak area by a factor of 1.79 can be seen in films deposited at 21 W. It is reported in [27] that the increase in D-peak intensity is associated with the growth of the number of C_6 molecules with sp^2-hybridized bonds.

The RS spectra also show the change of I_D/I_G as specified in the table. In pure films synthesized at 17.5 W, I_D/I_G is equal to 0.14, the increase in the plasma discharge power causes the increase in I_D/I_G to 0.19, i.e. an increase in I_D/I_G indicates an increase in the number of C_6 molecules. With the introduction of 3.5 at.% iridium at the synthesis powers of 17.5 W and 21 W, I_D/I_G ratio increases from 0.5 to 0.75, respectively. The I_D/I_G ratio increases with an increasing number of C_6 rings within the cluster and a decreasing fraction of chain-like groups [28]. This is because peak D is associated with atom ordering in an amorphous structure, and peak G is associated with structure disordering. The presented studies have demonstrated that iridium influences the formation of the local atomic structure of DLC films.

In RS spectra for DLC films, FWHM of G-peak is an important parameter that provides the information about structural and defect characteristics of a material. A decrease in the FWHM of the G-peak indicates an increase

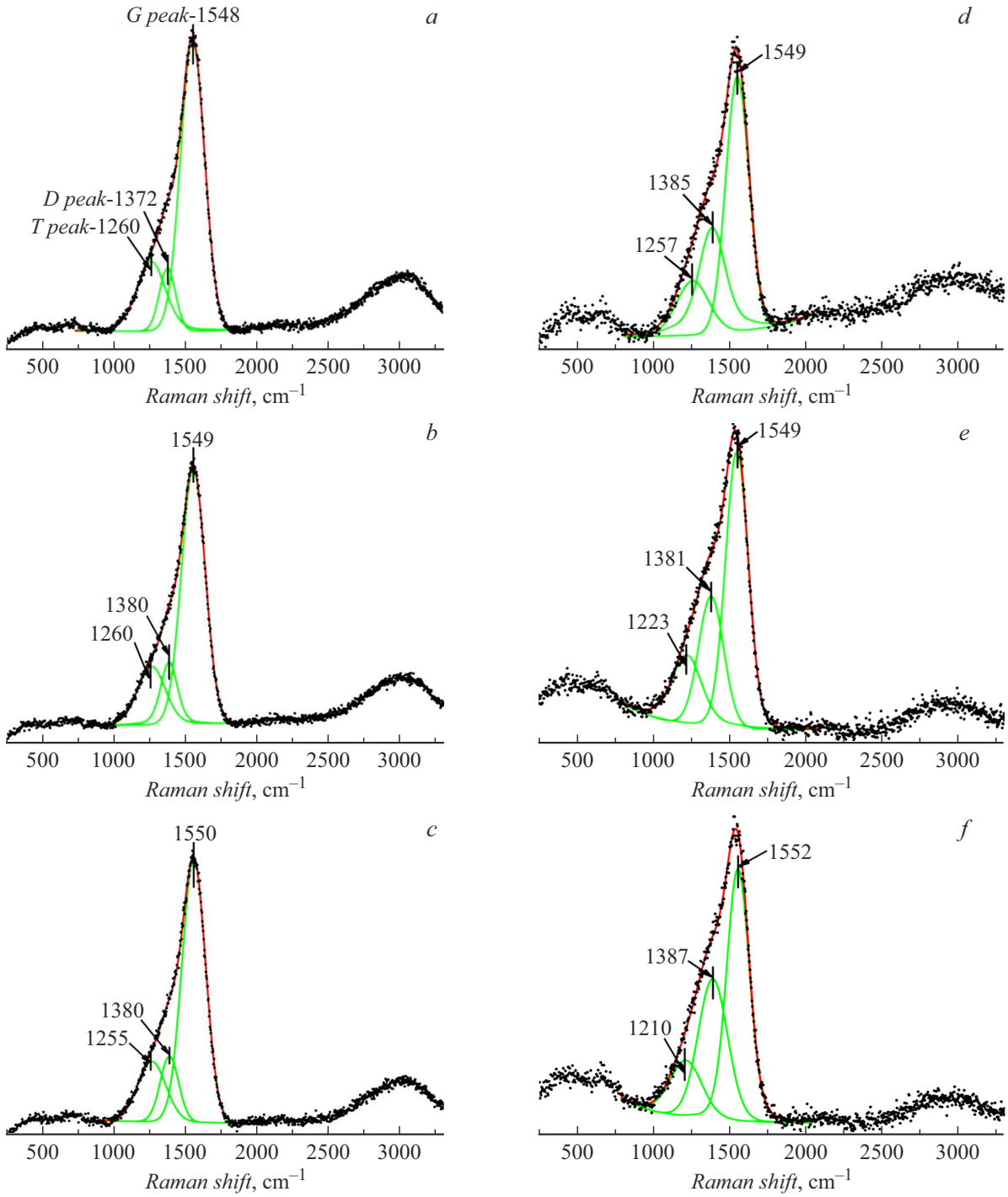

Figure 4. Raman scattering of DLC films arranged by the Voigt method: *a*–*c* — DLC films without iridium deposited at 17.5 W, 19.25 W, 21 W; *d*–*f* — DLC films with $X_{\mathrm{Ir}} \sim 3.5$ at.% deposited at 17.5 W, 19.25 W, 21 W.

in the size of ordered structures, which may consist of both sp^2- and sp^3-sites. For films synthesized with increasing DC discharge power, both pure and iridium-doped, the FWHM(G) peak values decrease accordingly by 21, 19 and 23 cm^{-1}, as shown in the table.

Examination of RS using different lasers (473 and 633 nm) also gave the calculated dispersion of G-peak ($dispG$) [29,30]. The G-peak position also increases as the excitation wavelength decreases. In [30], dispersion of G-peak was defined as function of rate of change of the G-peak position in the excitation wavelength using equation (1). Change of $dispG$ indicates the change of sp^2/sp^3-hybridization ratio. Figure 5 shows the change of G-peak dispersion depending on the iridium concentration in films deposited at different powers:

Dependence of I_D/I_G and FWHM of G-peak on the iridium concentration in DLC films

Plasma discharge power, W	$X_{Ir} = 0.00$ at.%		$X_{Ir} = 3.5$ at.%		Δ FWHM (G)
	FWHM of G-peak, cm^{-1}	I_D/I_G	FWHM of G-peak, cm^{-1}	I_D/I_G	
17.5	198	0.14	177	0.5	21
19.25	195	0.19	174	0.63	21
21	193	0.19	170	0.75	23

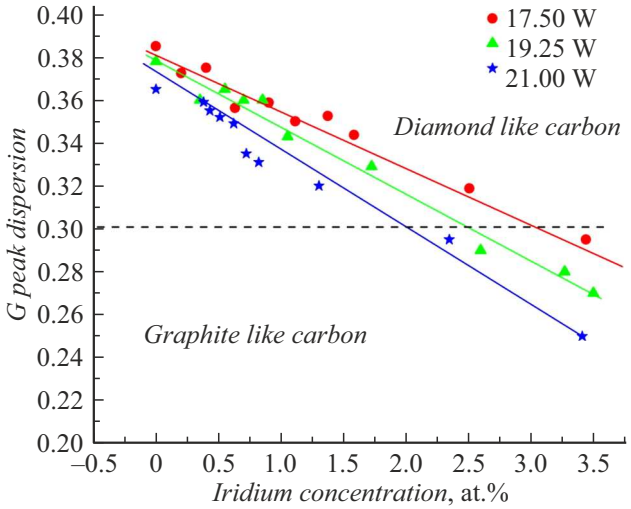

Figure 5. Dispersion of G-peak of DLC films depending on the iridium concentration and plasma discharge power.

$$G\,disp\left(\frac{\mathrm{cm}^{-1}}{\mathrm{nm}}\right) = \frac{G_{pos}\,(473\,\mathrm{nm}) - G_{pos}\,(633\,\mathrm{nm})}{(633-473)\,\mathrm{nm}}. \quad (1)$$

Calculation of $dispG$ shows (equation (1)) that the increase in iridium concentration causes a decrease in $dispG$ from 0.38 to $0.25\,\mathrm{cm}^{-1}\cdot\mathrm{nm}^{-1}$, and such variation is observed at different synthesis powers. According to the data presented in [29], a $dispG$ value below $0.3\,\mathrm{cm}^{-1}\cdot\mathrm{nm}^{-1}$ indicates an increase in the number of sp^2 sites and a higher content of hexagonally ordered carbon atom ring clusters within the amorphous matrix. At a value $dispG \geq 0.3\,\mathrm{cm}^{-1}\cdot\mathrm{nm}^{-1}$, the film is dominated by sp^3-hybridized carbon atoms. The maximum change in $dispG$ is observed at a DC discharge power of 21 W during synthesis.

3. Optical properties

The size of the graphitic clusters can be estimated using the value of the I_D/I_G ratio. According to [27], the authors associate the intensity ratio of the D and G peaks in the Raman spectrum with the linear size L_a of graphitic clusters. In an earlier study [31], the cluster sizes in the synthesized films were determined to range from 6 to 12 Å, and therefore, using equation (2), the size of the graphitic inclusions L_a in the diamond-like carbon film matrix was estimated in accordance with [27]:

$$\frac{I_D}{I_G} = C_1(\lambda)L_a^2, \quad (2)$$

where $C_1(\lambda)$ is the parameter that depends on the light wavelength.

Equation (2) was used to calculate the cluster dimensions that varied in the range from 6 Å to 13 Å depending on the iridium concentration and synthesis power. The change of carbon cluster dimensions and iridium concentration affects the distribution of density of electron states and, consequently, the conductivity and optical properties.

The value of the optical band gap (E_g), calculated from the transmission and reflection spectra, is a structure-sensitive parameter. Thus, it is possible to carry out an evaluation of the sp^2/sp^3 hybridization ratio depending on E_g. E_g of amorphous DLC films is much smaller than that of diamond (~ 5 eV) because the density of band-edge electron states is formed by π-electrons of sp^2 sites [32]. Transitions between allowed states define the optical properties and band gap.

Figure 6 shows the effect of plasma discharge power on transmission spectra of both pure and iridium-containing DLC films. Figure 6, *a* shows that the highest transparency is observed in a DLC film deposited at 17.5 W. An increase in discharge power to 21 W leads to a decrease in the transmission spectra. In the spectral range from 200 to 1100 nm, the light transmittance of films synthesized at a power of 17.5 W decreases from 84% to 22%. As the synthesis power increases by 3.5 W, the transmission decreases from 77 to 16%. Compared with a pure film, iridium-doped films shown in Figure 6, *b* have a lower transparency in this spectrum range. In the same spectrum range, the transmission of films with iridium nanoparticles deposited at 17.5 W varies from 51 to 6%. As the plasma discharge power increases to 21 W, the transmission decreases from 44 to 6%.

In [31] E_g was calculated in the region where the absorption coefficient $\alpha \sim 10^5\,\mathrm{cm}^{-1}$. Dependence of absorption on transmitted light energy obeys absorption square law:

$$\alpha h\nu \sim (h\nu - E_g)^2. \quad (3)$$

As is known [33,34], extrapolation of the linear dependence of $\sqrt{\alpha h\nu}$ on the abscissa axis $h\nu$ makes it possible

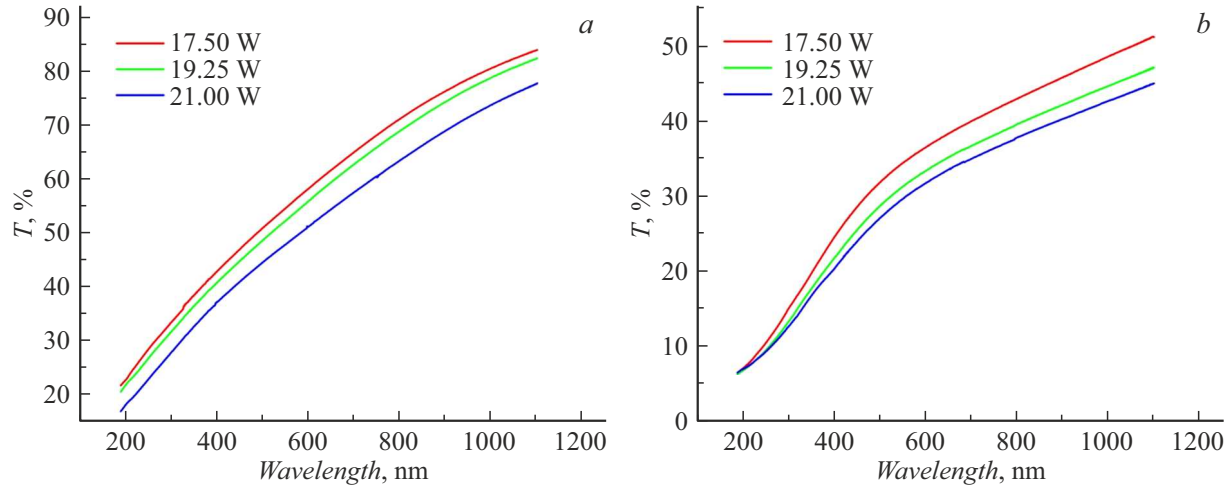

Figure 6. Transmission spectra of DLC films synthesized at different discharge powers, X_{Ir}, at.%: *a* — 0.00, *b* — 3.50 ± 0.03.

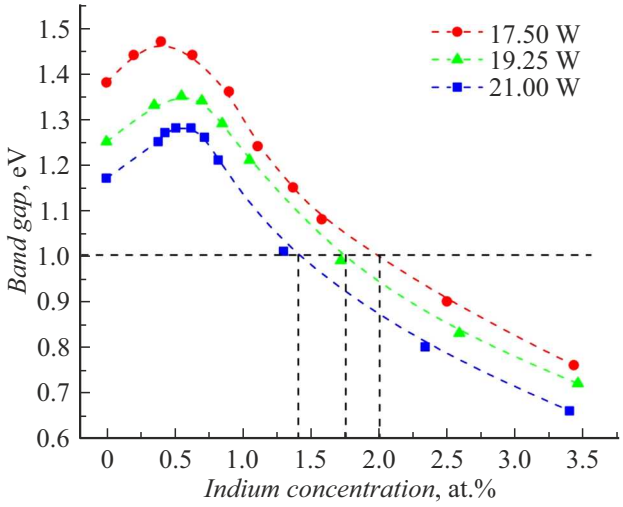

Figure 7. Dependence of E_g on iridium concentration and synthesis power.

to determine the band gap width E_g. Dependence of the band gap on the iridium concentration and discharge power is shown in Figure 7. In pure samples, as the discharge power increased from 17.5 to 21 W, E_g varied from 1.38 to 1.17 eV, respectively. The introduction of iridium up to approximately 0.42 at.% at a power of 17.5 W leads to an increase in the band gap width to 1.46 eV. A similar picture is also observed at the synthesis powers of 19.25 W and 21 W. It should be noted that an increase in power leads to a greater change in E_g, and at 21 W the change in E_g amounts to 0.11 eV. Such increase in the band gap indicates that the density of band-edge electron states changes. A similar behavior was observed in a-C:H⟨Sn$_x$⟩ films with increasing tin concentration up to ∼ 1 at.% [35].

Thus, the variation of the concentration of occupied π-states of carbon sp^2sites depends considerably on the concentration and free energy states 5*d* of the iridium shell. It is presumably more advantageous for iridium nanoparticles with small concentrations to form a simple cubic structure rather than a face-centered cubic (FCC) lattice. This may give rise to a change of the distribution of density of electron states in iridium. Therefore, it is possible that at low concentrations, the unfilled 5*d* states of the iridium electronic shell lie energetically below the occupied π-states of the carbon sp^2 sites. Therefore, it is energetically favorable for a π-electron to transition to free 5*d* level of iridium, thereby filling the state. This gives rise to a change of the density of electron states and band gap broadening. Further increase in the iridium concentration causes a smooth drop of E_g. This change of E_g is probably associated with the formation of a particular concentration of sp^2 sites as well as of iridium nanoparticle sizes. Increase in sp^2 sites, as proved by the RS spectra decomposition, gives rise to an increase in the concentration of occupied π states. In addition, the increase in the iridium nanoparticle sizes forms a FCC structure where the 5*d* shell is energetically comparable and even larger in energy than the density of states with the formed sp^2 sites. In materials with high concentration of sp^2 clusters, the band gap decreases because the density of π — occupied, π^* — unoccupied states increases. It was reported in [27] that an increase in the sp^2 site content leads to a decrease in the band gap width. Iridium nanoparticles are also involved additionally in the band structure formation. With the maximum concentration of iridium ∼ 3.5 at.%, decrease in the band gap to 0.75 and 0.65 eV is observed at the synthesis power of 17.5 W and 21 W, respectively.

4. Electrical properties

DLC films are typically characterized by high specific electrical resistivity, ranging from 10^2 to $10^{11}\,\Omega\cdot$cm, depending on the deposition method and synthesis conditions [36,37]. The electrical resistivity of DLC films can

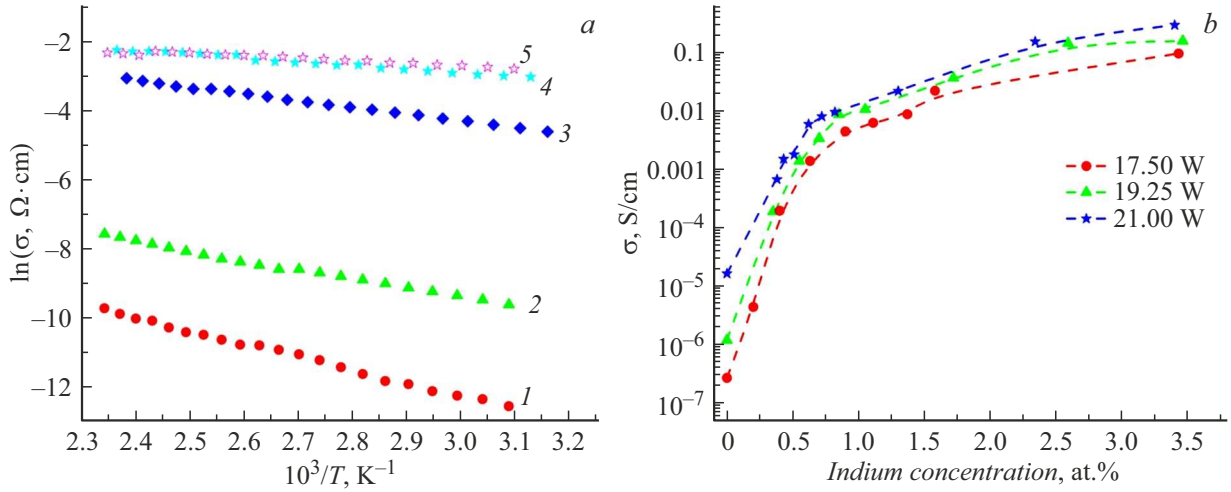

Figure 8. *a* — dependences of conductivity on temperature at the DC discharge power of 17.5 W (X_{Ir}, at.%: *1* — 0.00, *2* — 0.63, *3* — 1.11, *4* — 2.5, *5* — 3.43), *b* — dependences of conductivity on iridium concentration in DLC⟨Ir⟩ films fabricated at different DC discharge powers.

be reduced by several orders of magnitude by incorporating metals or metal nanoparticles into the films. Conductivity is defined by complex interaction between sp^2- and sp^3-hybridized bonds and the presence of various structural defects and clusters. DLC films with a high content of sp^2 sites form graphite-like clusters, in which π-electrons are free and become conduction electrons with a lower activation energy. Such clusters form conductive paths in the matrix. The calculated dimensions of nanoclusters consisting of sp^2 sites vary with the synthesis conditions and iridium concentration. Increase in the synthesis power and iridium concentration causes an increase in the dimensions of a nanocluster consisting of sp^2 sites. Nanoclusters consisting of sp^2 sites and iridium nanoparticles are conductivity islands in the amorphous diamond-like carbon matrix with sp^3-hybridization of C−C bonds. In such an amorphous DLC film, both hopping and tunneling conductivity can occur between the conductive nanoparticles and nanoclusters. As has been determined, the temperature dependence of conductivity obeys the Arrhenius law, i.e.

$$\sigma = \sigma_0 \exp\left[-\frac{E_\sigma}{kT}\right]. \qquad (4)$$

The activation conductivity mechanism takes place in DLC⟨Ir⟩ films, as mentioned above, the band gap varies from 0.6 eV to 1.5 eV depending on the iridium concentration. As an example, Figure 8, *a* shows $\ln(\sigma) = f(1000/T)$ that confirms the exponential behavior of conductivity. The temperature dependence of conductivity in Figure 8, *a* is shown for films deposited at the DC discharge power of 17.5 W.

This work studied the conductivity (σ_r) at 300 K. Dependence of σ on the iridium concentration is shown in Figure 8, *b*, where it can be seen that the concentration dependence of DLC film conductivity varies exponentially rather than linearly. Such exponential conductivity variation is described by the percolation conductivity mechanism [16,38,39]. As shown in Figure 8, *b*, in DLC⟨Ir⟩ films synthesized at the DC discharge power of 17.5 W, dependence of σ_r on the iridium concentration in the range from 0 to 0.9 at.% shows significant increase in the conductivity by a factor of $\sim 10^5$. Synthesis of DLC⟨Ir⟩ films at the DC discharge powers of 19.25 W and 21 W gives rise to a change of conductivity by a factor of $\sim 10^4$ and $\sim 10^3$, respectively. A further increase in iridium concentration from 0.9 to 3.5 at.% leads to a saturation of conductivity values, and σ gradually increases by an order of magnitude to approximately ~ 0.1 S/cm. Thus, a change in conductivity from $\sim 2 \cdot 10^{-7}$ to 0.1 S/cm is observed over the iridium concentration range up to 3.5 at.%, i.e., by approximately $\sim 10^6$ times.

Thus, the synthesis conditions and iridium affect the conductivity. Increase in the number of sp^2 sites causes the increase in the dimensions of clusters that serve as conductive pathways for electrons. Moreover, iridium nanoparticles are also involved in the charge carrier transfer.

Conclusion

The work studies the local structure and electronic properties of amorphous DLC films with iridium nanoparticles synthesized in different conditions. Scanning electron microscopy has shown that iridium is included in the carbon matrix in the form of isolated nanoparticles. The size and number of iridium nanoparticles increases as the concentration grows. The RS analysis has shown that the increase in plasma discharge power gave rise to the increase in sp^2 sites, but the formation of sp^2 site clusters during synthesis is affected more significantly by iridium nanoparticles. Band gap of amorphous DLC⟨Ir⟩ films has

been determined and the influence of iridium atoms on the formation of density of band-edge electron states has been shown. Moreover, the work shows considerable change of conductivity of the synthesized amorphous DLC⟨Ir⟩ films that is described by the percolation conductivity mechanism. Thus, it is shown that the structure and electronic properties of amorphous diamond-like thin films can be affected significantly.

Funding

The study was funded by the Committee of Science of the Ministry of Science and Higher Education of the Republic of Kazakhstan (grant №AP19676270).

Conflict of interest

The authors declare no conflict of interest.

References

[1] J. Robertson. Phys. Stat. Sol. (A), **205** (9), 2233 (2008). https://doi.org/10.1002/pssa.200879720
[2] A.I. Okhapkin, P.A. Yunin, E.A. Arkhipov, S.A. Kraev, S.A. Korolev, M.N. Drozdov, V.I. Shashkin. FTP, **54** (9), 865 (2020) (in Russian). DOI: 10.21883/FTP.2020.09.49822.14
[3] V.A. Vlasenko, S.N. Belyaev, A.G. Efimov, E.A. Ilyichev, M.D. Malenkovich, V.E. Nemirovsky, E.A. Poltoratsky, A.V. Goryachev, A.F. Popkov, G.V. Frolova, M.L. Shulepin, Pis'ma v ZhTF, **35** (15), 105 (2009) (in Russian).
[4] M.S. Dresselhaus, G. Dresselhaus, P.C. Eklund. *Science of Fullerenes and Carbon Nanotubes* (Academic Press, London, 1996)
[5] K.S. Novoselov, D. Jiang, F. Schedin, T.J. Booth, V.V. Khotkevich, S.V. Morozov, A.K. Geim. Proc. Nat. Acad. Sci. U.S.A., **102** (30), 10451 (2005). https://doi.org/10.1073/pnas.0502848102
[6] D. Li, N. Kong, R. Li, B. Zhang, Y. Zhang, Zh. Wu, Q. Zhang. Surf. Topography: Metrology and Properties, **9** (4), (2021). DOI: 10.1088/2051-672X/ac4086
[7] P.A. Radi, L. Vieira, P. Leite, V.J. Trava-Airoldi, M. Massi, D.A.P. Reis. Surface Topography: Metrology and Properties, **12** (1), 10 (2024). DOI: 10.1088/2051-672X/ad2ebe
[8] Kunming Gu, Yi Zheng, Junxuan Luo, Xiande Qin, Xinge Yang, Nadeem Abbas, Jiaoning Tang. Mater. Res. Express, **6** (8), 2019. DOI: 10.1088/2053-1591/ab197b
[9] Yeong Ju Jo, Teng Fei Zhang, Myoung Jun Son, Kwang Ho Kim. Appl. Surf. Sci., **433**, 1184 (2018). DOI: 10.1016/j.apsusc.2017.10.151
[10] Shuling Zhang, Shuaizheng Wu, Tenglong Huang, Xiangdong Yang, Feng Guo, Bo Zhang, Wenjie Ding. Coatings, **13** (10), 1743 (2023). https://doi.org/10.3390/coatings13101743
[11] Haibo Sun, Lv Yang, Huaichao Wu, Limei Zhao, Bin Ji. Appl. Surf. Sci., **641**, 158545 (2023). https://doi.org/10.1016/j.apsusc.2023.158545
[12] A.F. Yetim, H. Kovacı, A.E. Kasapoğlu, Y.B. Bozkurt, A. Çelik. Diamond and Related Mater., **120**, 108639 (2021). https://doi.org/10.1016/j.diamond.2021.108639
[13] A. Modabberas, P. Kameli, M. Ranjbar, H. Salamati, R. Ashiri. Carbon, **94**, 485 (2015). https://doi.org/10.1016/j.carbon.2015.06.081
[14] B. Pandey, S. Hussain. J. Phys. Chem. Solids, **72** (10), 1111 (2011). https://doi.org/10.1016/j.jpcs.2011.06.003
[15] B. Ghos, F. Guzmán-Olivos, R. Espinoza-González. Mater. Sci., **52**, 218 (2017).
[16] A.P. Ryaguzov, R.R. Nemkayeva, N.R. Guseinov, A.R. Assembayeva, S.I. Zaitsev. J. Non-Crystalline Solids, **532**, 119876 (2020). https://doi.org/10.1016/j.jnoncrysol.2019.119876
[17] F. Bekmurat, R.R. Nemkayeva, N.R. Guseinov, M.M. Myrzabekova, A.P. Ryaguzov. Mater. Today: Proceed., **25**, 13 (2019). https://doi.org/10.1016/j.matpr.2019.10.129
[18] Elnaz Mohammadini, Seyed Mohammad Elahi, Sheila Shahidi. Mater. Sci. Semicond. Process., **74**, 7 (2018). https://doi.org/10.1016/j.mssp.2017.10.003
[19] Raviraj Vankayala, Ganesh Gollavelli Badal Kumar Mandal. J. Mater. Sci.: Mater. Med., **24**, 1993 (2013). DOI: 10.1007/s10856-013-4952-z
[20] A.L. Ivanovsky. Uspekhi khimii **78**, (4) (2009) (in Russian).
[21] A. Modabberasl, P. Kameli, M. Ranjbar, H. Salamati, R. Ashiri. Carbon, **94**, 485 (2015). https://doi.org/10.1016/j.carbon.2015.06.081
[22] R.A. Alawajji, G.K. Kannarpady, Z.A. Nima, N. Kelly, F. Watanabe, A.S. Biris. Appl. Surf. Sci., **437**, 429 (2018). https://doi.org/10.1016/j.apsusc.2017.08.058
[23] A.I. Okhapkin, M.N. Drozdov, P.A. Yunin, S.A. Kraev, D.B. Radishchev. FTP, **57** (5), 309 (2023) (in Russian). DOI: 10.21883/FTP.2023.05.56195.09k
[24] P.A. Yunin, A.I. Okhapkin, M.N. Drozdov, S.A. Korolev, E.A. Arkhipov, S.A. Kraev, Yu.N. Drozdov, V.I. Shashkin, D.B. Radishchev. FTP, **54** (9), 855 (2020) (in Russian). DOI: 10.21883/FTP.2020.09.49820.12
[25] J. Robertson. Semicond. Sci. Technol., **18**, 12 (2003). DOI: 10.1088/0268-1242/18/3/302
[26] J. Robertson. Mater. Sci. Eng. R, **37** (4–6), 129 (2002). https://doi.org/10.1016/S0927-796X(02)00005-0
[27] A.C. Ferrari, J. Robertson. Phys. Rev. B., **61** (20), 14095 (2000). https://doi.org/10.1103/PhysRevB.61.14095
[28] F.C. Tai, S.C. Lee, C.H. Wei, S.L. Tyan. Mater. Transactions, **47** (7), 1847 (2006). DOI: 10.2320/matertrans.47.1847
[29] C. Casiraghi, F. Piazza, A.C. Ferrari, D. Grambole, J. Robertson. Diamond & Related Mater., **14**, 1098 (2005). DOI: 10.1103/PhysRevB.72.085401
[30] J. Robertson, A.C. Ferrari. Phil. Trans. R. Soc. Lond. A, **362**, 2477 (2004). https://doi.org/10.1098/rsta.2004.1452
[31] A.P. Ryaguzov, R.R. Nemkaeva, O.I. Yukhnovets, N.R. Guseinov, S.L. Mikhailova, F. Bekmurat, A.R. Asembaeva. Opt. i spektr., **127** (2), 251 (2019) (in Russian). DOI: 10.21883/OS.2019.08.48037.33-19
[32] J. Robertson, E.P. O'Reilly. Phys. Rev. B, **35** (6), 2946 (1987).
[33] K.V. Shalimova, *Fizika poluprovodnikov* (Energoatomizdat, M., 1985), 392 s. (in Russian).
[34] J. Tauc. Prog. Semicond., **9**, 89 (1965).
[35] A.P. Ryaguzov, R.R. Nemkaeva, N.R. Guseinov. FTP, **52** (10), 1207 (2018) (in Russian). DOI: 10.21883/FTP.2018.10.46463.8785
[36] A. Grill. Thin Solid Films, **355–356**, 189 (1999). https://doi.org/10.1016/S0040-6090(99)00516-7

[37] E. Staryga, G.W. Bąk. Diamond Related Mater., **14** (1), 23 (2005). https://doi.org/10.1016/j.diamond.2004.06.030
[38] B.I. Shklovski, A.L. Efros. Adv. Phys. Sci., **18** (11), 24 (1975). DOI: 10.1070/PU1975v018n11ABEH005233
[39] V.I. Roldughin, V.V. Vysotskii. Prog. Org. Coat., **39** (2–4), 81 (2000). https://doi.org/10.1016/S0300-9440(00)00140-5

Translated by E.Ilinskaya